

Bifurcation into shear bands on the Bishop and Hill polyhedron Part III: Case of the edges of dimension one

M. DARRIEULAT ⁽¹⁾, G. DAMAMME ⁽²⁾

⁽¹⁾ SMS, R3M, UMR CNRS 5146,
Ecole Nationale Supérieure des Mines de Saint-Etienne,
158 cours Fauriel, 42023 Saint-Etienne cedex 2, France

⁽²⁾ DM, DAM, Commissariat à l'Energie Atomique,
Le Ripault, 37260 Monts, France

THE PRESENT PAPER ends a series of three papers devoted to the micro-mechanical conditions which render possible the appearance of shear bands in crystalline materials. It presents the results on the edges of dimension 1 (encompassing the states of the deviatoric stress applied between two vertices of the Bishop and Hill polyhedron). They show that bifurcation is possible with a relatively small number of active slip systems, in conditions of strain hardening which are of the same order of magnitude as those at the vertices. An application is given to the case of the C {112} <11 $\bar{1}$ > oriented single crystal compressed in a channel die. The characteristic experimental feature: appearance of two successive sets of bands (111) [11 $\bar{2}$] and (11 $\bar{1}$) [112] is explained in terms of the most favoured bifurcation planes and the local rotation of the crystal. Though convincing to predict the onset of shear bands, the above calculations do not provide a description of their intergranular development, especially crossing of the grain boundaries, since at this stage the material has been too much affected by the intense shearing to be treated by a method of bifurcation.

Key words: shear bands, edges of dimension one, C {112} <11 $\bar{1}$ > orientation.

Notations

q	respective contribution of the vertices of an edge $d = 1$ to the state of deviatoric stress,
θ	inclination of the {hkh}<uuv> crystallographic orientations around $[\bar{1}10]$, measured from the C {112} <11 $\bar{1}$ > orientation,
ED	elongation direction,
$\dot{\gamma}_P$	glide rate common to two coplanar (CP) slip systems,
$\dot{\gamma}_D$	glide rate common to two codirectional (CD) slip systems,
ξ	normalised shear strain,
B_i	apex on the stereographic projection of a flow cone,
G_s	source grain,
G_t	target grain,
\mathbf{L}	fourth order three-dimensional tensors,
h_B	microscopic strain-hardening modulus in a shear band,
τ_c^B	critical resolved shear stress on a shear band,
h^{gk}	element of the matrix of microscopic heterogeneous strain hardening.

1. Introduction

THE PRESENT ARTICLE ends a sequence of papers [1, 2] devoted to shear banding on the Bishop and Hill polyhedron, conducted with Hill and Hutchinson's approach of bifurcation. This phenomenon was seen as a dramatic change in the glide rates on the slip systems, and the recombination of some of them into an intense shearing. When they are scarce, in the case of the edges $d = 2$ or 3, only specific geometries lead to bifurcation. On the contrary, the 'vertex effect' was explained by their large number (six or eight).

The case of the 216 edges of dimension $d = 1$, with four, five or six available slip systems, is intermediary, and allows to take the full measure of the 'edge effect'. It corresponds to states of deviatoric stress with one degree of freedom between two end vertices \mathbf{S}^{ν_1} and \mathbf{S}^{ν_2} which can be written as:

$$\mathbf{S} = q\mathbf{S}^{\nu_1} + (1 - q)\mathbf{S}^{\nu_2}, \quad 0 \leq q \leq 1.$$

Table 1. States of deviatoric stress in the eight classes of edges $d = 1$.

$$\begin{bmatrix} 2q & 0 & 0 \\ 0 & -q & 6 - 6q \\ 0 & 6 - 6q & -q \end{bmatrix}$$

Edge n°1 class 3A,
(from 4A to 4C)

$$\begin{bmatrix} 3 + q & 3 - 3q & 0 \\ 3 - 3q & -3 + q & 0 \\ 0 & 0 & -2q \end{bmatrix}$$

Edge n°7 class 3B,
(from 4A to 4E)

$$\begin{bmatrix} 0 & q & q \\ q & 0 & 2 - q \\ q & 2 - q & 0 \end{bmatrix}$$

Edge n°19 class 3C,
(from 4B to 4C)

$$\begin{bmatrix} 2 - 2q & 3 & 3 \\ 3 & -1 + q & 3q \\ 3 & 3q & -1 + q \end{bmatrix}$$

Edge n°31 class 3D,
(from 4B to 4D)

$$\begin{bmatrix} -2 + 2q & 3 & 3 \\ 3 & 1 - q & 3q \\ 3 & 3q & 1 - q \end{bmatrix}$$

Edge n°43 class 3E
(from 4B to 4D)

$$\begin{bmatrix} -1 + q & 3 - 3q & 0 \\ 3 - 3q & 2 - 2q & 3 + 3q \\ 0 & 3 + 3q & -1 + q \end{bmatrix}$$

Edge n°55 class 3H,
(from 4C to 4D)

$$\begin{bmatrix} 0 & 0 & 0 \\ 0 & 1 - q & 1 + q \\ 0 & 1 + q & -1 + q \end{bmatrix}$$

Edge n°79 class 3G
(from 4C to 4E)

$$\begin{bmatrix} 3 - q & 3 & 3q \\ 3 & -3 + 2q & 0 \\ 3q & 0 & -q \end{bmatrix}$$

Edge n°85 class 3H,
(from 4D to 4E)

Examples taken in each of the eight crystallographic classes 3A to 3H are given in Table 1. They are labelled according to [3] and other articles referenced in the previous papers. The class of their end vertices (4A to 4E) has also been tabulated. Interest is raised by two types of considerations. One is that the C (Copper)-oriented crystals, with their transparent geometry of four symmetric slip systems, are known for their aptness to shear banding and have been much used for the experimental investigation in high stacking fault energy metals [4]. The other is the success of the relaxed constraint hypothesis in modelling of the polycrystals [5] which implies such stress states and has also been applied to the appearance of shear bands [6]. Hence the tree parts below: the resolution of the (S) system (see [1], Eqs. (3.9)), which requires here a special treatment because of its nonlinearity; its application to the case of single crystals which, like the C orientation, retain a symmetry plane during their deformation; and brief considerations on crossing of the grain boundaries.

2. Resolution of the system (S) on the edges $d = 1$

2.1. Algebra

For the resolution of the system (S), the normal ν to the plane of bifurcation is taken as a data, and $C_{ij} = R(\alpha_{ij} + \lambda\beta_{ij}) + \gamma_{ij}$. (S) is uniquely determined for all the edges $d = 1$ which belong to classes other than 3B and 3H. For the latter, a choice has to be made of four independent slip systems for Eqs. (3.9)₅ to (3.9)₉ which assure that the proposed bifurcation shear belongs to the vectorial space which comprises the flow cone. Along with Eq. (3.9)₄, they form a homogeneous linear system (S') of six equations with seven unknowns η_i , $i = 1..3$ and μ_j , $j = 1..4$. Since those quantities are defined only within a scalar factor, (S') gives the direction of the flow whatever q if ν is known. It is important to note that the deviatoric stress state does not intervene in (S'), which corresponds to purely geometrical conditions, but only in the equilibrium equations (3.9)₁ to (3.9)₃. So, along one edge, the planes of bifurcation and their associated directions are the same from one end to the other.

When the η_i , $i = 1..3$ are determined as a solution of the system (S'), the equilibrium conditions form a system of three equations with the unknowns y , R and λ . It is not homogeneous because of the γ_{ij} , and the R and λ are uniquely determined, meanwhile y is determined within the accuracy of scaling factor, the same as for the η_i . For two opposite deviatoric stress states (taken on edges numbered v and $v + 108$), $R(\mathbf{S}) = -R(-\mathbf{S})$. The consequences on the most and least favoured bifurcation shear systems are the following. The extreme values of R vary along the edges, as can be seen in Fig. 1, where they have been represented as a function of the parameter q . $R_{\max}(\mathbf{S}) = -R_{\min}(-\mathbf{S})$ and $R_{\min}(\mathbf{S}) = -R_{\max}(-\mathbf{S})$.

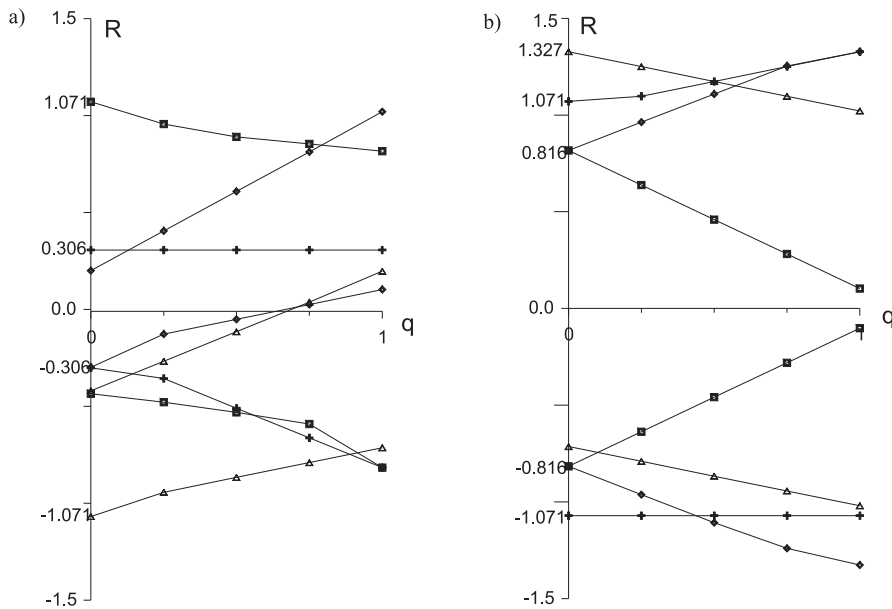


FIG. 1. Extreme values of R along the edge $d = 1$.

(a) Classes 3A to 3D; (b) Classes 3E to 3H,

Classes 3A and 3E +, Classes 3B and 3F \diamond , Classes 3C and 3G \square , 3D and 3H \triangle .

Contrary to what happens at the vertices, in most cases, $R_{\max} \neq R_{\min}$. So, each graph corresponds to one half of the edges of a given class. On one particular edge, the resolution of (S) yields the $(hkl) [uvw]$ corresponding to R_{\max} and the $(h'k'l')[u'v'w']$ corresponding to R_{\min} . In most cases, there are one, two or four flow directions associated with each extreme value. Along one edge, the $(hkl) [uvw]$ and the $(h'k'l')[u'v'w']$ are identical. So here they are referred to infra as the most/least favoured bifurcating systems of the edge. If the opposite edge is considered, the most favoured systems of the first become the least favoured ones of the opposite and vice-versa. When all the edges of one class are considered, these systems form crystallographically equivalent sets $\{hkl\} \langle uvw \rangle$ and $\{h'k'l'\} \langle u'v'w' \rangle$ which are alternatively maximum and minimum for one half the edges of the class. They are given in this form in the developments below.

The largest value found for R_{\max} is 1.327 in the classes 3E, 3F and 3H. Many extreme values already shown in the second paper of this series, such as 0.306, 0.816 and 1.071, appear again in the calculations, because they correspond to the same combinations of active slip systems. In spite of the lesser number of available slip systems, the bifurcation on the edges $d = 1$ is as easy as at the vertices from the point of view of the strain hardening.

As in the case of the vertices, the normals to the bifurcating planes form cones in the Euclidian space, or continuous domains on a stereographic projection, limited by apices with simple Miller indices: $\{100\}$, $\{110\}$, $\{111\}$, $\{112\}$ and $\{113\}$. For lack of space, all these cones have not been drawn here, but a specimen can be found infra: see Fig. 3. When only four slip systems are available, if all the μ_j are of the same sign, the shear flow solution of the system (S') belongs to the flow cone of the edges. It is not true in the case of the classes 3B and 3H. For them, the cone has to be divided into sub-cones formed by four independent slip systems, which are tested till one of them (if any) contains the proposed shear flow. There are twelve sub-cones of dimension four for the class 3B and five for the class 3H. The percentage of planes on which the bifurcation is possible has also been calculated in Table 2. It shows that only the classes 3C and 3E offer large possibilities for the bifurcation.

Table 2. Percentage of bifurcation according to the crystallographic class.

Class	3A	3B	3C	3D	3E	3F	3G	3H
Percentage of bifurcating planes	4.4	2.1	15.0	1.4	22.5	4.5	1.6	3.0

2.2. Results for the eight classes of edges

The analytical expression of the η_i as a function of the ν_i is given by the resolution of the system (S') as a quotient of polynomials of degree two in ν_i . Due to the fact that the η_i are significant only within a scaling factor, simplifications can be obtained and, with the exception of the classes 3F and 3G, the η_i can be given as linear expressions of the ν_i . The extrema of R are found in three typical situations: i) for a combination of CP (coplanar) or CD (codirectional) slip systems, as at the vertices ii) on some single slip system, which remains active alone while the others stop gliding iii) by an exchange between the plane and the direction of shear in some slip system, so that the bifurcation produces a $\{110\}\langle 111\rangle$ shear.

Examples are given in the following analysis of the various classes.

Class 3A: two sets of CP slip systems; the η_i are $\langle \nu_1, \nu_1, \nu_2 - \nu_3 \rangle$; hence, the flow direction belongs to the $\{110\}$ planes of the crystal, a feature common to several classes below. The most/least favoured shear systems are the $\{111\}\langle 112 \rangle$, obtained by combination of two CP systems, and $\{110\}\langle 111 \rangle$, which corresponds to the situation iii) supra. At the end vertices, the bifurcation with only four slip systems is obtained for the characteristic values $R_{\max} = 0.306$ and $R_{\min} = 0.816$.

Class 3B: six slip systems forming, as a whole, two sets of CP and two sets of CD systems. The shear direction is $\langle \nu_1, \nu_1, \nu_2 + \nu_3 \rangle$. The R_{\max} and R_{\min} all

correspond to $\{110\}\langle 111\rangle$. Unlike the class 3A, there are several combinations leading to this result.

Class 3C: the four slip systems form two sets of CP and two sets of CD systems, the shear direction is $\langle \nu_1 + \nu_2, \nu_1 + \nu_3, \nu_2 - \nu_3 \rangle$. The extreme values of R correspond to $\{111\}\langle 110\rangle$ and $\{113\}\langle 112\rangle$. The latter is the result of combinations of the type:

$$3(\bar{1}\bar{1}1)[\bar{1}0\bar{1}] + 2(\bar{1}11)[110] \rightarrow (113)[\bar{1}\bar{2}1].$$

Class 3D: the four slip systems form two sets of CP but only one set of CD systems. The η_i are $\langle \nu_1, \nu_1, \nu_2 - \nu_3 \rangle$ as in the class 3A, with the same the most/least favoured slip systems. It must nevertheless be noted that the cones of the normals to the bifurcating planes are not identical, and involve the apices $\{113\}$ in the class 3D along with the apices $\{110\}$ and $\{111\}$. Only the latter two appear with the class 3A.

Class 3E: there is one set of CP and one set of CD systems. The η_i are $\langle \nu_1, \nu_1, \nu_2 + \nu_3 \rangle$, as in the class 3B. The extreme values of R are found for $\{111\}\langle 112\rangle$, by the combination of two CP systems, and $\{110\}\langle 111\rangle$. One edge belonging to this class is studied with more details in Sec. 2.

Class 3F: this class has a set of two CP slip systems, one of them being CD with a third one; the fourth one has no particular property. The shear direction is a quadratic expression of the ν_i . On the whole edge, $R_{\max} = -R_{\min}$ and the corresponding shear systems are $\{110\}\langle 111\rangle$ and $\{111\}\langle 110\rangle$; this phenomenon of exchange of the Miller indices between the shear plane and the shear direction, which is the rule with the vertices, is found for the edges $d = 1$ only with the classes 3F and 3G.

Class 3G: the four slip systems are neither CP or CD. The class 3G has much of the bifurcating characteristics of the class 3F. The shear directions are also a quadratic expression of the ν_i , but belong to the $\{110\}$ crystal planes. The extreme values of R are different: 0.102 and 0.816 for 3F, instead of 0.816 and 1.327 (absolute maximum) for 3G.

Class 3H: the five slip systems form two sets of CP, the fifth system has no particular properties; all their shear directions are different. The η_i are $\langle \nu_1, \nu_1, \nu_2 + \nu_3 \rangle$, as in the classes 3B and 3E. All the most/least favoured bifurcation systems are of the $\{110\}\langle 111\rangle$ type.

The above analysis has been done in the axes of the crystal, while the boundary conditions are applied to the sample and expressed in its reference frame. Hence, the frequency with which the classes 3A...3H are solicited cannot be determined *a priori*: it depends on the mechanical agency and the crystal orientations. As seen above, the eight classes are unequally likely to bifurcate. So, the study concentrates now on a particular case, which activates the class 3E, and

has been chosen because of its aptness to bifurcation and the numerous experimental results available as a test.

3. The case of the channel die compression of a C{112}<111>crystal

3.1. Characteristics of the deformation of the C single crystal

When a single crystal of Copper orientation is compressed in a channel-die, its lattice rotates around the transverse $[\bar{1}10]$ direction, either towards the orientation (001) $[110]$, described as Cube rotated 45° around the normal direction, or the Goss orientation (110) $[00\bar{1}]$: see [7]. This phenomenon has been documented both at the macroscopic level, using X-ray diffraction [8], and at the microscopic one, using the EBSD (Electron Back Scattering Diffraction) or the CBED (Convergent Beam Electron Diffraction) techniques [9]. Let ED, TD and ND be respectively the elongation, transverse and normal directions of the channel die, also referred to as 1, 2 and 3 in the expression of the tensors. Throughout the deformation path, the plane (ED, ND), being a $\{110\}$ plane, remains an element of symmetry for both the mechanical agency and the crystal, whose position can be determined by the angle θ between ND and its $[001]$, as sketched in Fig. 2. The latter has been drawn with TD pointing towards the sheet of paper, to ensure that ED, TD and ND form a direct reference frame. The C orientation (112) $[11\bar{1}]$ thus corresponds to $\theta = -35.26^\circ$. The crystal rotates positively (+) TD towards the Dillamore (4 4 11) $[11\ 11\ \bar{8}]$, the (116) $[33\bar{1}]$ and the Cube rotated 45° ND orientations; it rotates (-)TD towards (111) $[11\bar{2}]$ and Goss. The deformation is generally accompanied by a shear D_{EN} small with respect to the compressive deformation ($D_{EN} = \xi\dot{\epsilon}$) so that the strain rate tensor in the axes of the die is:

$$D = \dot{\epsilon} \begin{bmatrix} 1 & 0 & \xi \\ 0 & 0 & 0 \\ \xi & 0 & -1 \end{bmatrix}, \quad |\xi| \ll 1.$$

When expressed in the axes of the crystal as a function of θ , the strain-rate tensor takes the characteristic form $\mathbf{D} = [D_{ij}]$ with $D_{11} = D_{12} = D_{22}$ and $D_{13} = D_{23}$ for all θ and ξ . This means that all the \mathbf{D} can be accommodated by slip systems with only two different glide rates. Since $\{110\}$ is an element of symmetry, four of them are active. So, all along the deformation path, the flow rate belongs to a vectorial subspace $d = 4$, and the corresponding deviatoric stress state is on an edge $d = 1$. These edges, which vary with the angle θ and the quantity ξ , have been reported on Fig. 2 in the case $\xi = 0$. A simple method for their determination consists in calculating the vertices at which the work rate

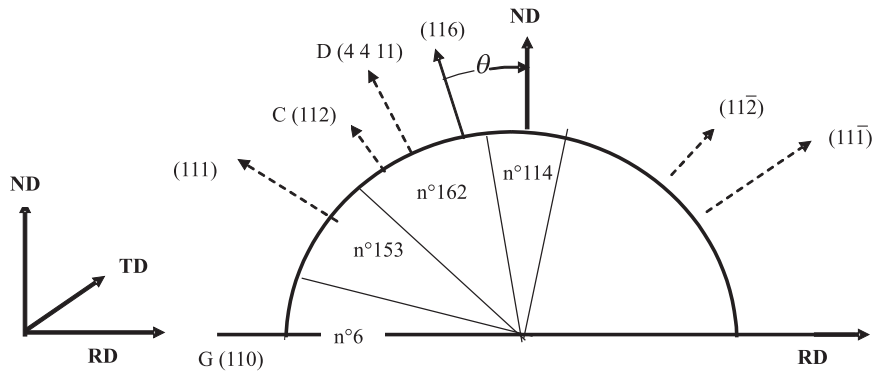


FIG. 2. Rotation of the crystal lattice around TD.

is maximum. There are two of them at a time, and the relevant edge is formed by the deviatoric stress states between them. Here are some of their characteristics:

- For $-45^\circ < \theta < -9.73^\circ$, in the range of the C, Dillamore and $(116)[33\bar{1}]$ orientations, the edge is $n^\circ 162$ (class 3E). There are two CP active systems $(111)[01\bar{1}]$ and $(111)[10\bar{1}]$ and two CD ones $(\bar{1}11)[\bar{1}\bar{1}0]$ and $(1\bar{1}1)[\bar{1}\bar{1}0]$. If $\dot{\gamma}_P$ and $\dot{\gamma}_D$ are the glide rates on the CP and CD systems, equating the macroscopic and microscopic expressions of the tensor \mathbf{D} leads to:

$$(3.1) \quad \begin{aligned} \dot{\gamma}_P &= \frac{\sqrt{6}}{2} \dot{\epsilon} (\cos 2\theta + \xi \sin 2\theta) \quad \text{with} \quad \dot{\gamma}_P \geq 0, \\ \dot{\gamma}_D &= \frac{\sqrt{6}}{4} \dot{\epsilon} \left[\cos 2\theta + 2\sqrt{2} \sin 2\theta + \xi \left(-\sin 2\theta + 2\sqrt{2} \cos 2\theta \right) \right] \\ &\quad \text{with} \quad \dot{\gamma}_D \geq 0. \end{aligned}$$

It can be checked that if $\xi = 0$, these quantities are positive for $-45^\circ < \theta < -9.73^\circ$.

- For $-80.27^\circ < \theta < -45^\circ$, the edge is $n^\circ 153$ (also class 3E). When submitted to (-) TD rotations from an initial C orientation, the crystals enter this range which comprises in particular $(111)[11\bar{2}]$ and has the same CD systems as the edge $n^\circ 162$, but different CP, namely $(11\bar{1})[101]$ and $(11\bar{1})[011]$. As will be seen infra, this has important consequences on the bifurcation into shear bands.

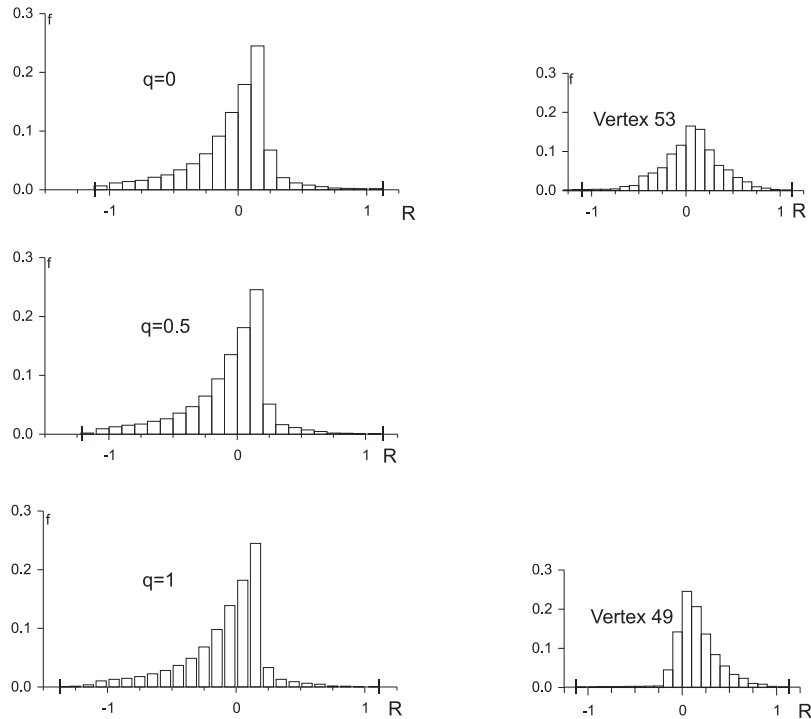
- Around $\theta = 0^\circ$ (Cube rotated 45° ND) the edge is $n^\circ 114$; around $\theta = -90^\circ$, it is the opposite one, edge $n^\circ 6$. They belong to the class 3A, characterized by two sets of CP slip systems.

The corresponding deviatoric stress states can be calculated as seen in Sec. 1 with the help of the parameter q . On the edge $n^\circ 162$ for example, $\mathbf{S} = q\mathbf{S}^{53} + (1 - q)\mathbf{S}^{49}$ with $0 \leq q \leq 1$. In the reference frame of the sample, taking into account that $T_{11} = 0$, the stress tensor is:

Table 3. Remarkable bifurcation shear systems on the edge n°162.

q	Shear system	$R = h_a/\tau_c$				
		0	1/4	1/2	3/4	1
B_1	(111) [11 $\bar{2}$]			1.071		
B_1^*	(11 $\bar{2}$) [111]			-1.071		
B_2	(001) [$\bar{1}\bar{1}0$]			0.186		
B_2^*	($\bar{1}\bar{1}0$) [001]			-0.186		
B_3	(121) [11 $\bar{3}$]	0.393	0.403	0.413	0.423	0.433
B_4	($\bar{1}12$) [110]	0.196	0.245	0.294	0.342	0.391
B_5	(10 $\bar{1}$) [111]	-1.296	-1.221	-1.148	-1.076	-1.003

The histograms of the R values for all the possible planes of bifurcation have also been drawn: they depend on the parameter q . Figure 4 pictures the following: i) $q = 0$, the deviatoric stress state at the vertex 53 ii) $q = 1/2$ iii) $q = 1$, stress state at the vertex 49. For i) and iii), the R values were also calculated as in [2], that is, taking into account the six active slip systems of the end vertices instead of the four available on the edge n°162. Not surprisingly, the bifurcation is easier when more slip systems are available.

**FIG. 4.** Histogram of R from one vertex to the other on the edge n° 162.

The exceptional aptitude of the C orientation to shear banding comes from the fact that the micro-shear bands have no difficulty to develop into macroscopic ones since the most favoured shear systems remain so in spite of the lattice rotation. And it proves that propagation is possible when only four active slip systems are available.

4. Considerations on crossing of the grain boundaries

The previous sections of this series of papers have dealt about the way shear bands appear within grains. Many authors [12] have shown that most of them originate in coarsening of slip systems already active during the homogeneous phase of the deformation. In the above analysis, this corresponds to the intensification of the glide on some systems as the result of the bifurcation. As long as the crystallographic orientation is maintained, the conditions of existence of the band are met and this can explain its propagation without deflection within the grain, although other approaches of the post-bifurcation development are possible [13, 14, 15]. Do the above calculations cast light on what happens at the grain boundaries since the shear bands, in rolling for example, can end up as macro-bands expanding throughout the whole thickness of the sheet?

4.1. Experimental observations

First, let the main observations done on this phenomenon be mentioned [16]. Once formed, the bands propagate rapidly within the grains. The shear reaches high values, typically $\bar{\varepsilon} = 5$ or more, as can be seen by the displacement of the bars of the microgrids when observing micro-displacements at the surface of a sample [17]. Various authors have pointed out the specificity of this mechanism, which involves a rarefaction of the dislocations within the microband, in which the mean free path of the existing ones increases [18]. A parallel was done with the easy glide which can be found at the onset of the tensile deformation of crystals oriented so that only one slip system is active. The micro-band can even be considered as a specific slip system with a large, although instable Burgers vector [19].

The crossing of the grain boundaries takes place later in the process, after intragranular microbands parallel to the initial one have developed. The propagation is delayed at the grain boundary, against which the dislocations pile up so that the band gains impetus to channel through the neighbouring grain [20]. A distinctive feature of the phenomenon is that a band seldom changes its plane at the crossing, as shown by numerous electron microscopy observations. There is no experimental evidence of changes in the direction of shear, although the contrary has not been documented either. This rectitude is all the more remarkable since neighbouring grains are randomly and largely disoriented in

polycrystals, and since the dependence of shear banding on the crystallography is well established.

4.2. Discussion on the mechanism of shear banding in the target grain

The following development is an attempt to apply the mechanical analysis of the initiation of shear bands to their propagation from a source grain G_s to a target one G_t . Since the plane is the same and the respective crystallographic orientations are arbitrary, the calculations can be conducted according to the scheme used above, based on the system (S) . The normal ν is considered as a data which can take any value in the Euclidian space. Differential equilibrium must be met in all cases. The deviatoric state of stress in G_s gives little information on the corresponding state in G_t , even if the equilibrium through the grain boundary is supposed. Hence all the varieties on the Bishop and Hill polyhedron are possible in the target grain. The strain hardening in it increases with the deformation; since the crossing of the grain boundary occurs with delay, R takes a range of values while the band is held at the frontier, so that R must be considered as an adjustable parameter. It will be necessary later to verify that the values suitable for the system (S) fall in the range in which the bifurcation is possible: see Table 2 in [2] and Table 2 in the present paper. Two different assumptions are used for the discussion:

- the direction of the shear η is the same in G_s and G_t , hence it must be checked that the η_i , $i = 1..3$ satisfy all the equations of (S) ,
- η is free, and the η_i , $i = 1..3$ are considered as unknowns.

In both cases, the strongest hypothesis made is the following: can the shear originated in the grain G_s propagate in G_t through the work of a suitable combination of the slip systems available in G_t , or is the propagation due to a quite distinct mechanism? Counting the unknowns and the parameters in the system (S) gives some clues.

i) η is considered as a data. Since $\nu\eta = 0$, the system (S) reduces to eight equations. Whatever the dimension d of the variety, there are only seven unknowns and parameters: y proportional to the gradient of the rate of hydrostatic pressure, the $\mu_1 \dots \mu_{(5-d)}$ which assure the compatibility of the flow, the parameters $\lambda_1 \dots \lambda_d$ of the rate constitutive law and R which represents the strain hardening. In the general case, no solution is available. This means that if the direction of the shear is kept constant between the grains G_s and G_t , it is not possible to retain all the hypotheses of the bifurcation.

ii) the η_i , $i = 1..3$ are considered as three unknowns. As in the previous sections of these papers, (S) can be analysed as a homogeneous linear system of $(9 - d)$ unknowns depending upon $(d + 1)$ parameters, hence solutions exist in certain cases provided that:

- The shear band waits at the grain boundary until the target grain takes the value required for R . The parameter R decreases all along the deformation path and this could explain the delay for the crossing,

- The μ_i are such that the flow belongs to the cone of the normals, and not only to \mathcal{E}_V . This is a restrictive condition, as shown in [1]. The abovementioned Tables (2) give the percentage of planes which actually bear a shear direction in the cases $d = 0$ (vertices) and $d = 1$ (edges) according to the crystallographic class. In no case it exceeds 26% of the planes of the Euclidian space. Since the grains along a macro shear band are randomly oriented, how is it possible to explain that the band is not stopped at some grain boundary? The cases $d > 1$ are not favourable either, because the last five equations in (S) involve only $(8 - d)$ unknowns $\eta_i, i = 1..3, \mu_1 \dots \mu_{(5-d)}$ and no parameter (see analysis in [1]).

Hence, even if no condition of continuity of the flow direction is set between the grains G_s and G_t , the hypothesis according to which the shear band in the target grain is the product of the activity of the slip systems of the original crystal cannot be maintained. Although the band is formed in the matrix and retains its chemical composition, it must be considered as a solid with different mechanical properties. It can be represented by a crystalline medium with only one slip system of a new type, to which the following rate constitutive law can be attributed:

$$(4.1) \quad \check{\mathbf{S}}^* = \frac{h_B}{\tau_c^B} \left(\left(\mathbf{S}_0 + \sum_{n=1}^4 \lambda^n \mathbf{X}^n \right) \otimes \mathbf{S}_0 \right) : \mathbf{D},$$

where h_B is the microscopic strain hardening modulus (lower than in an ordinary slip system) τ_c^B the critical resolved shear stress and \mathbf{S}_0 the projection of the origin. As pointed out supra, the physics of the intense deformation in the shear band, with the alteration it causes to the sub-structure of the material, supports this point of view.

5. General conclusion

The conditions in which the homogeneous flow of a rigid plastic, rate-insensitive crystal whose yield surface is a Bishop and Hill polyhedron gives way to shear banding, have been studied by adapting a bifurcation analysis by Bishop and Hill (1975). For this purpose, the rate-constitutive law of the crystal has been explicated. Its form depends on the applied state of deviatoric stress, i.e. on the variety of the Bishop and Hill polyhedron. A distinctive feature is that, for the edges on which exist non-zero vectorial subspaces orthogonal to the flow, it involves parameters which are not determined by constitutive (but rather here, by equilibrium) considerations.

The vertices and the edges $d = 1$ deserve a special interest because shear banding is possible on a continuum of planes, each of them bearing a single direction of shear and associated to one state of strain hardening (represented by the parameter R). Those which are possible first have been determined in the case of the channel die compression. The predicted geometry is in good agreement with the experimental results, in particular with the characteristic slant of about 35° to the rolling direction. The strain hardening at the onset of the shear banding corresponds to what actually happens in the most sensitive alloys (e.g. Al-Mg or some austenitic steels).

The mechanical analysis only predicts the possibility of localization; its implementation in the metal is linked to substructural events which control the movement of the dislocations, like the breakdown of the obstacle networks. Although designed at the mesoscopic scale (fraction of μm), the present theory takes into account the occurrence of such microscopic phenomena, since it analyses the loss of homogeneity as a change in the glide rates on the active slip systems; but it does not necessitate a precise description of the physical causes of this transformation. It is consistent with the fact that shear bands appear at quite different stages in materials with a similar initial flow behaviour. It also explains that the present calculations work well to predict the appearance of the shear bands, but are not relevant for their development, especially the crossing of grain boundaries.

The study above has been done assuming a uniform strain hardening, because its heterogeneity entails that every flow surface is a particular case, so that the results would lack generality. Nevertheless, uniformity is a strong hypothesis: the effects of latent hardening have been put into evidence in shear banding metals and might be at the origin of the blockade of some slip systems, hence of the bifurcation phenomena. When a general incremental strain hardening law $\dot{\tau}_c^g = \sum_{k=1}^{(5-d)} h_{gk} \dot{\gamma}^k$ is considered, it is easier to calculate the rate constitutive law than in the case of the Bishop and Hill polyhedron because the strain hardening relation can be inverted (see Appendix). Most of the results should be similar to those obtained previously in the homogeneous case. The choice of physically founded values to model anisotropic strain hardening and its application to specific deformation paths is a task to be set about soon.

Appendix A.

For rigid plastic rate-insensitive crystals deforming under the Schmid law on an arbitrary set of slip systems, the flow surface is a polyhedron in the five-dimensional vectorial space of the states of deviatoric stress. In the general case all the τ_c^g are different. For f.c.c. crystals for example, there is a maximum of 24

facets, since some of them may be situated outside the polyhedron because their τ_c^g is high.

The number of vertices also depends on the τ_c^g . In the f.c.c. case it is, in general, larger than 56 (which corresponds to the Hill and Hutchinson polyhedron) because there are no symmetries, and each vertex has only 5 active slip systems. In the same way, the edges are more numerous, but each corresponds to $(5 - d)$ slip systems.

The piecewise-linear differential constitutive law:

$$(A.1) \quad \check{\mathbf{S}}^* = \mathbf{L} : \mathbf{D}$$

where \mathbf{L} is a fourth order three-dimensional tensor which depends on the variety of the flow surface. As seen before, arbitrary parameters λ^n , $n = 1..d$ associated to tensors \mathbf{X}^n such as $\mathbf{X}^n : \mathbf{D} = 0$ intervene in it.

The calculations presented in the case of the Bishop and Hill polyhedron can be reproduced provided that the active slip systems are known by their Schmid factors \mathbf{M}^{sg} $g = 1..(5 - d)$. The calculation of \mathbf{L} in Eq. (6) is simpler than in [1] because, if there are no particular symmetries, the differential hardening law can be inverted:

$$(A.2) \quad \dot{\gamma}_g = \sum_{k=1}^d h_{gk}^{-1} \dot{\tau}_c^k$$

hence:

$$(A.3) \quad \mathbf{D} = \sum_{g=1}^d \mathbf{M}^{sg} \dot{\gamma}_g = \sum_{g=1}^d \mathbf{M}^{sg} \sum_{k=1}^d h_{gk}^{-1} \dot{\tau}_c^k = \sum_{g=1}^d \mathbf{M}^{sg} \left(\sum_{k=1}^d h_{gk}^{-1} \mathbf{M}^{sk} : \check{\mathbf{S}}^* \right).$$

Since the \mathbf{M}^s are symmetric tensors, \mathbf{L} has the symmetries of the elasticity and for practical purposes, the rate constitutive law can be written as:

$$(A.4) \quad \check{\mathbf{S}}^* = \left(\left(\mathbf{A} + \sum_{n=1}^d \lambda^n \mathbf{X}^n \right) \otimes \mathbf{B} \right) : \mathbf{D},$$

\mathbf{A} and \mathbf{B} being symmetric second order tensors such as $\mathbf{A} \otimes \mathbf{B} = \left[\sum_{g,k=1}^d h_{gk}^{-1} \mathbf{M}^{sg}$

$$\otimes \mathbf{M}^{sk} \right]^{-1}.$$

This allows to calculate all the elements of a system of the same form as the system (S) in [1] and results similar to the isotropic hardening case are expected. The number of unknowns and parameters is the same and depends on

the dimension of the variety, hence a range of bifurcating cases should appear if $d < 2$. Conclusions on crossing of the grain boundaries similar to those drawn in the present paper have been presented in the case of heterogeneous strain hardening [21].

Acknowledgment

The authors are greatly indebted to Professor H. Paul for communicating his and his Polish colleagues' experience on the conditions in which the shear bands appear and develop in single crystals.

References

1. M. DARRIEULAT, A. CHENAOUI, *Bifurcation into shear bands on the Bishop and Hill polyhedron, Part I: General analysis*, Arch. Mech., **56**, 2, 137–156, 2004.
2. M. DARRIEULAT, D. CHAPELLE, *Bifurcation into shear bands on the Bishop and Hill polyhedron. Part II: Case of the vertices*, Arch. Mech., **56**, 6, 453–472, 2004.
3. U.F. KOCKS, H. CHANDRA, *Slip geometry in partially constrained deformation*, Acta Metall., **30**, 695–709, 1982.
4. Z. JASIEŃSKI, T. BAUDIN, A. PIĄTKOWSKI, R. PENELLE, *Orientation changes inside shear bands occurring in channel-die compressed (112)[$\bar{1}\bar{1}$] copper single crystals*, Scripta Mater., **35**, 3, 397–403, 1996.
5. Y.S. LIU, L. DELANNAY, P. VAN HOUTTE, *Application of the Lamel model for simulating cold rolling texture in molybdenum sheet*, Acta Mater., **50**, 7, 1849–1856, 2002.
6. G.R. CANOVA, U.F. KOCKS, M.G. STOUT, *On the origin of shear bands in textured polycrystals*, Scripta Metall., **18**, 437–442, 1984.
7. R. BECKER, J.F. BUTLER, H. HU, L.A. LALLI, *Analysis of an aluminium single crystal with unstable initial orientation (001)[110] in channel die compression*, Metall. Trans. A, **22A**, 45–58, 1991.
8. G.D. KÖHLHOFF, A.S. MALIN, K. LÜCKE, M. HATHERLY, *Microstructure and texture of rolled {112}<111> copper single crystals*, Acta Metall., **36**, 10, 2841–2847, 1988.
9. K. MORII, H. MECKING, Y. NAKAYAMA, *Development of shear bands in f.c.c. single crystals*, Acta Metall., **33**, 3, 379–386, 1983.
10. P. WAGNER, O. ENGLER, K. LÜCKE, *Formation of Cu-type shear bands and their influence on deformation and texture of rolled f.c.c. (112)[$\bar{1}\bar{1}$] single crystals*, Acta Metall. Mater., **43**, 10, 3799–3812, 1995.
11. H. PAUL, M. DARRIEULAT, A. PIĄTKOWSKI, *Local orientation changes and shear banding in {112}<111> oriented aluminium single crystals*, Z. Metallkd., **92**, 1213–1221, 2001.
12. A. KORBEL, *The model of microshear banding in metals*, Scripta Metall. Mater., **24**, 1229–1238, 1990.
13. S. YANG, C. REY, *Shear band post-bifurcation in oriented copper single crystals*, Acta Metal. Mater., **42**, 8, 2763–2774, 1994.

14. H. PETRYK, K. THERMANN, *Post-critical deformation pattern in plane strain plastic flow with yield surface vertex effect*, Int. J. of Mech. Sci., **42**, 2133–2146, 2000.
15. R. B. PECHERSKI, *Modelling of large plastic deformations based on the mechanism of micro-shear banding: Physical foundations and theoretical description in plane strain*, Arch. Mech., **44**, 5–6, 563–584, 1992.
16. P. DUBOIS, M. GASPÉRINI, C. REY, A. ZAOUÏ, *Crystallographic analysis of shear bands initiation and propagation in pure metals, Part II: Initiation and propagation of shear bands in pure ductile rolled polycrystals*, Arch. Mech., **40**, 1, 35–40, 1988.
17. J.Y. POUSSARDIN, *Caractérisation et évolution des bandes de cisaillement dans les monocristaux d'Al-Mn (Characterisation and evolution of the shear bands in Al-Mn single crystals)*, PhD thesis, Ecole des Mines de Saint-Etienne (France) 2003.
18. Z.S. BASIŃSKI, S.J. BASIŃSKI, *Plastic deformation and work hardening*, [in:] Nabarro FRN, *Dislocations in Solids*, North Holland Publishing Company, **4**, 1979.
19. A. KORBEL, *Perspectives of the control of the mechanical performance of metals during forming operations*, J. Mater. Process. Tech., **34**, 41–47, 1992.
20. A. PAWELEK, A. KORBEL, *Soliton-like behaviour of moving dislocation group*. Phil. Mag. B, **61**, 829–837, 1990.
21. M. DARRIEULAT, A. CHENAOUÏ, *Analyse mécanique du franchissement des joints de grains par les bandes de cisaillement (Mechanical analysis of the crossing of grain boundaries by shear bands)*, [in :] Damil N. 6^{ème} congrès de mécanique, Tanger, Maroc, **1**, 82–83, 2003.

Received January 21, 2005.
